CHIN. PHYS. LETT. Vol. 36, No. 9 (2019) 097502

Magnetic and Magnetocaloric Properties of Polycrystalline and Oriented $Mn_{2-\delta}Sn$ *

Kun Li(李昆)[1,2], Fanggui Wang(王芳贵)[1,2], Youfang Lai(赖有方)[1,2], Mingzhu Xue(薛明珠)[1,2], Xin Li(李鑫)[1,2], Jinbo Yang(杨金波)[1,2,3], Changsheng Wang(王常生)[1,2], Jingzhi Han(韩景智)[1,2], Shunquan Liu(刘顺荃)[1,2], Wenyun Yang(杨文云)[1,2], Yingchang Yang(杨应昌)[1,2], Honglin Du(杜红林)[1,2]**

[1]*School of Physics, Peking University, Beijing 100871*
[2]*Beijing Key Laboratory for Magnetoelectric Materials and Devices, Beijing 100871*
[3]*Collaborative Innovation Center of Quantum Matter, Beijing 100871*

(Received 5 May 2019)

Mn-based Heusler alloys have attracted significant research attention as half-metallic materials because of their giant magnetocrystalline anisotropy and magnetocaloric properties. We investigate the crystal structure and magnetic properties of polycrystalline, [101]-oriented, and [100]-oriented $Mn_{2-\delta}Sn$ prepared separately by arc melting, the Bridgeman method, and the flux method. All of these compounds crystallize in a Ni_2In-type structure. In the $Mn_{2-\delta}Sn$ lattice, Mn atoms occupy all of the 2a and a fraction of the 2d sites. Site disorder exists between Mn and Sn atoms in the 2c sites. In addition, these compounds undergo a re-entrant spin-glass-like transition at low temperatures, which is caused by frustration and randomness within the spin system. The magnetic properties of these systems depend on the crystal directions, which means that the magnetic interactions differ significantly along different directions. Furthermore, these materials exhibit a giant magnetocaloric effect near the Curie temperature. The largest value of maximum of magnetic entropy change ($-\Delta S_{\rm M}$) occurs perpendicular to the [100] direction. Specifically, at 252 K, maximum $-\Delta S_{\rm M}$ is 2.91 and 3.64 $J{\cdot}kg^{-1}K^{-1}$ for a magnetic field of 5 and 7 T, respectively. The working temperature span over 80 K and the relative cooling power reaches 302 J/kg for a magnetic field of 7 T, which makes the $Mn_{2-\delta}Sn$ compound a promising candidate for a magnetic refrigerator.

PACS: 75.30.Gw, 75.30.Sg DOI: 10.1088/0256-307X/36/9/097502

In recent years, considerable attention has been paid to 'half-metallic' materials with complete spin polarization at the Fermi level ($E_{\rm F}$).[1–7] The Heusler alloys constitute a large family of half-metallic materials,[1,8–11] which may be divided into full-Heusler and half-Heusler alloys according to the number of atoms in the unit cell. The chemical formulas for these compounds are A_2BC and ABC, respectively, where A and B are transition-metal elements and C is a main-group element. In the half-Heusler alloys, their unit cell can be regarded as one A atom is replaced by a vacant site in the full-Heusler unit cell.[4,8]

As half-metallic Heusler alloys, Mn-based alloys with the non-cubic crystal structure have attracted significant attention. Some of these alloys have large magnetocrystalline anisotropy and high Curie temperature above room temperature,[12,13] while some have competing ferro-and-antiferromagnetic interactions between transition-metal moments located at different lattice sites.[14–16] In addition, because of their magnetocaloric effects, Mn-based alloys have also been extensively studied in the field of magnetic refrigeration. Due to a series of problems in traditional refrigeration technology (e.g., environmental pollution), many studies have focused on magnetic refrigeration, which is an emerging environmentally friendly refrigeration technology.[17–20]

In the study of the magnetocaloric effect of Mn-based alloys, there were some studies on $Mn_{2-\delta}Sn$ doped materials. Few previous reports have focused on the magnetic and magnetocaloric properties of $Mn_{2-\delta}Sn$. To better understand these materials, we systematically study the magnetic properties and magnetic interactions of single-phase polycrystalline, [101]-oriented and [100]-oriented samples of $Mn_{2-\delta}Sn$ alloys.

We prepared a polycrystalline sample of $Mn_{2-\delta}Sn$ with a nominal composition of $Mn_{1.9}Sn$ by arc melting under an Ar atmosphere. The purity of the constituent elements exceeded 99%, and the sample was vacuum annealed at 1123 K for three days. The [101]-oriented and [100]-oriented $Mn_{2-\delta}Sn$ samples were grown by the Bridgeman method and the flux method, respectively. The nominal composition of the polycrystalline sample, which was also the raw material of the Bridgeman method, was $Mn_{1.9}Sn$ while the ratio of Mn:Sn in the flux method was 1:2 (Sn is the flux). Room-temperature x-ray diffraction measurements were carried using an X'pert Pro MPD diffractometer (Cu K_α radiation, $\lambda = 1.54187$ Å) and confirmed that all the samples were single phase. The magnetization measurements were made by a conventional physical property measurement system (PPMS-

*Supported by the National Natural Science Foundation of China under Grant Nos 11675006, 51731001 and 11805006, and the National Key Research and Development Program of China under Grant Nos 2017YFA0206303, 2016YFB0700901 and 2017YFA0403701.
**Corresponding author. Email: duhonglin@pku.edu.cn
© 2019 Chinese Physical Society and IOP Publishing Ltd

9,2–350 K).

Although $Mn_{2-\delta}Sn$ is predicted to form either a cubic or hexagonal crystal structure, only the hexagonal $B8_2$ phase (a Ni_2In-type structure) with space group $p63/mmc$ (a = 4.37–4.40 Å, c=5.47–5.53 Å)[14,21–25] has been prepared experimentally.[26,27]

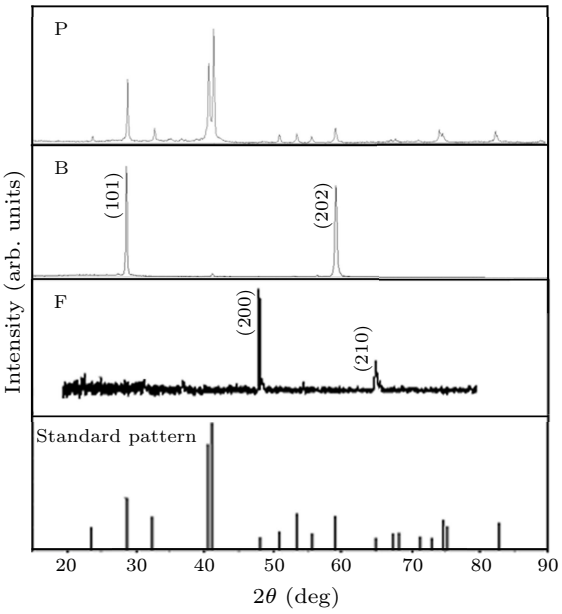

Fig. 1. X-ray diffraction patterns of P, B and F samples and of a standard sample.

The notations P, B and F indicate the samples prepared by arc-melting, the Bridgeman method and the flux method, respectively (the size of B is $2\times2\times1$ mm^3 and the size of F is $3\times1\times1$ mm^3). Figure 1 shows the x-ray diffraction patterns of the three different samples. The diffraction pattern produced by sample P can be indexed as a single phase of hexagonal Ni_2In-type structure. Rietveld refinement shows that, in the $Mn_{2-\delta}Sn$ lattice, Mn atoms occupy all Wyckoff 2a sites and a fraction of the 2d sites, and the 2c sites are randomly occupied by a small amount of Mn and all the Sn atoms. These results are consistent with those of the previous studies.[14,21–25] The refined lattice parameters for sample P are a=4.395(3) Å and c=5.520(1) Å.

By indexing the standard pattern, we find that (as expected) sample B grew along the [101] direction, which is parallel to the pulling direction of the Bridgman method. To investigate the magnetic properties of $Mn_{2-\delta}Sn$ in the [100] direction, we selected sample F, which grew primarily along the [100] direction (and slightly along the [210] direction), from hundreds of crystals. Since the (210) peak is very weak, we consider sample F to be oriented in the [100] direction.

Figure 2 shows the thermomagnetic curves (5–300 K in a field of 50 Oe) under zero-field-cooled (ZFC) and field-cooled (FC) conditions. In addition, sample B (F) was measured with an applied magnetic field parallel (denoted by Bp (Fp)) and perpendicular (denoted by Bv (Fv)) with respect to the [101] ([100]) direction, respectively.

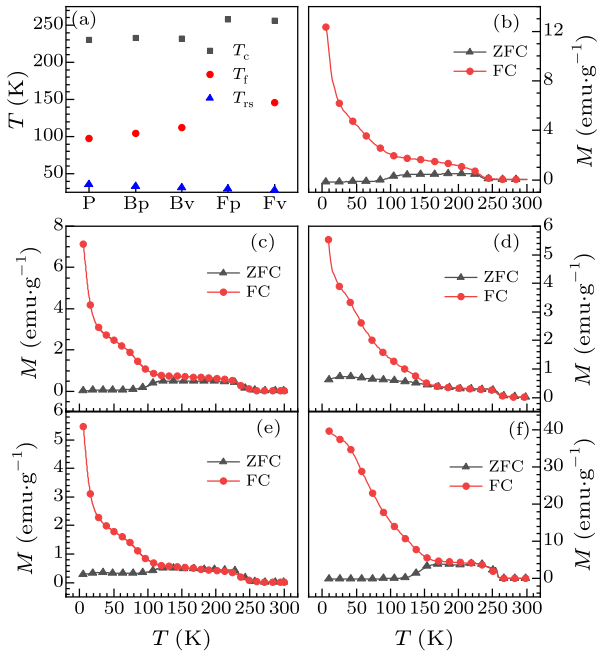

Fig. 2. (a) Magnetic transition temperature for different samples. Here T_C is the Curie temperature, T_f is the freezing temperature, and T_{rs} is the spin-reorientation transition temperature. (b)–(f) Thermomagnetic curves for different samples under an applied magnetic field of 50 Oe under ZFC and FC conditions. Panels (b)–(f) correspond to samples P, Bp, Fp, Bv and Fv, respectively.

The curves for sample P show three transition temperatures. The two higher transition temperatures (230 and 97 K) are considered to be the paramagnetic-to-ferrimagnetic transition temperature T_C (the minima in the $\partial M/\partial T$ curves) and the magnetic freezing temperature T_f (the maxima in the $\partial M/\partial T$ curves), respectively. The ferrimagnetic region is between the Curie temperature and the freezing temperature. The splitting between the ZFC and FC curves for sample P is ascribed to the pinning of domain wall.[28–30] The irreversibility of the M–T curve below T_f is due to the magnetic freezing effect, which is a characteristic of the spin-glass state. The transition from the ferrimagnetic state to the spin-glass state is called the re-entrant spin-glass-like transition.[27,31,32]

Table 1. Magnetic transition temperatures of different samples.

	T_c (K)	T_f (K)	T_{rs} (K)
P	230	97	35
Bp	233	104	33
Bv	232	112	31
Fp	258		29
Fv	256	146	28

The appearance of the re-entrant spin-glass-like transition may be caused by frustration (i.e., no spin configuration can satisfy all the magnetic couplings simultaneously and minimize the energy) and randomness within the spin system.[28] The frustration of the

spin systems originates from the geometric relation of the placements of the antiferromagnetic-coupled magnetic atoms. In the Ni_2In-type structure, Mn atoms in the octahedron ($2a$ sites) and triangle bipyramid ($2d$ sites) interact directly. Meanwhile, along the c axis, Mn atoms in $2a$ sites are arranged as linear chains, thus direct coupling occurs between spins. According to the curve of interaction energy versus Mn–Mn distance, the effective exchange integral between nearest-neighboring Mn atoms is negative (antiferromagnetic interaction). The nearest-neighboring $2a$ and $2d$ sites form a triangle so that the magnetic moments of antiferromagnetic coupling cannot be antiparallel with respect to any nearest-neighbor magnetic moment, which causes frustration. The randomness comes from the disordered arrangement of the atoms and holes within the Mn $2d$ sublattice. The spin-reorientation transition appears at the lowest transition temperature (about 35 K). The magnetic transitions in the Bp, Bv, Fp and Fv samples are similar to those in sample P, but the transition temperatures differ. Table 1 lists the transition temperatures of all the samples. As can be seen from Table 1, Fp does not have a freezing temperature, which shows that no re-entrant spin-glass-like transition occurs because there is no frustration in the [100] direction. Meanwhile, the freezing temperatures T_f in the Bp, Bv, and Fv samples (104, 112 and 146 K, respectively) are significantly greater than that in sample P (97 K). Samples Bp and Bv have almost the same Curie temperature (233 and 232 K, respectively) as Fp and Fv (258 and 256 K, respectively), although sample F has a Curie temperature higher than sample P (230 K). In addition, the magnetic moments in sample F mostly focus on the Fv direction, as determined by comparing the results of Fp and Fv at 20 K (5.52 emu/g for Fp and 39.72 emu/g for Fv). Fv has a larger magnetic susceptibility, indicating that this direction may be the direction in which the net magnetic moment is arranged, which means that it is easy to magnetize in the direction of Fv. This conclusion is also confirmed in Fig. 3, which shows that Fv thoroughly saturates at 5000 Oe, whereas Fp saturates at 10000 Oe.

Figure 3 shows the M–H loops for the samples at different temperatures with an applied magnetic field of up to 8 T. The magnetization of all the oriented samples is well saturated in a field of 1 T, whereas sample P approaches saturation. However, the saturation magnetization differs significantly for the samples with different orientations. The saturation magnetization of Fp is the largest and reaches 72.6 emu/g. Sample Fv is the easiest to saturate (the saturation field is 5000 Oe), and sample Bv is the hardest to saturate (the saturation field is 1 T), which indicates anisotropy. Furthermore, almost no magnetic hysteresis appears except for Bv at 20 K, which indicates that $Mn_{2-\delta}Sn$ undergoes a second-order magnetic transition.

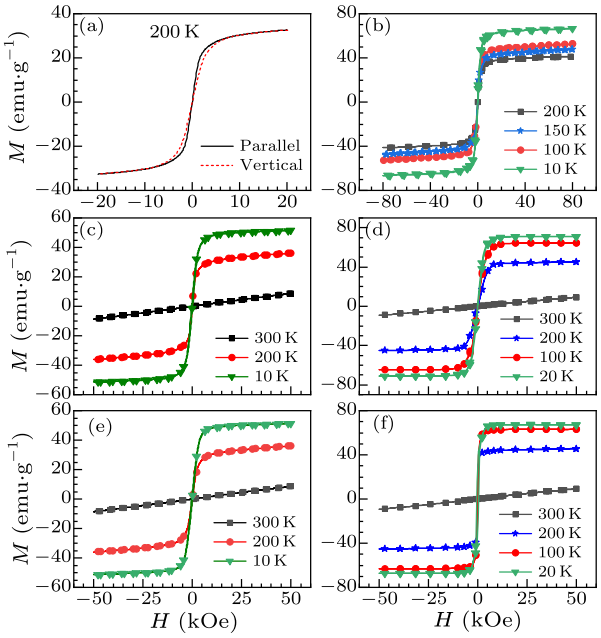

Fig. 3. (a) The M–H loops of Bp and Bv at 200 K with an applied magnetic field up to 2 T (Bv is harder to saturate than Bp). (b)–(f) The M–H loops of different samples at different temperatures. Panels (b)–(f) correspond to samples P, Bp, Fp, Bv and Fv, respectively.

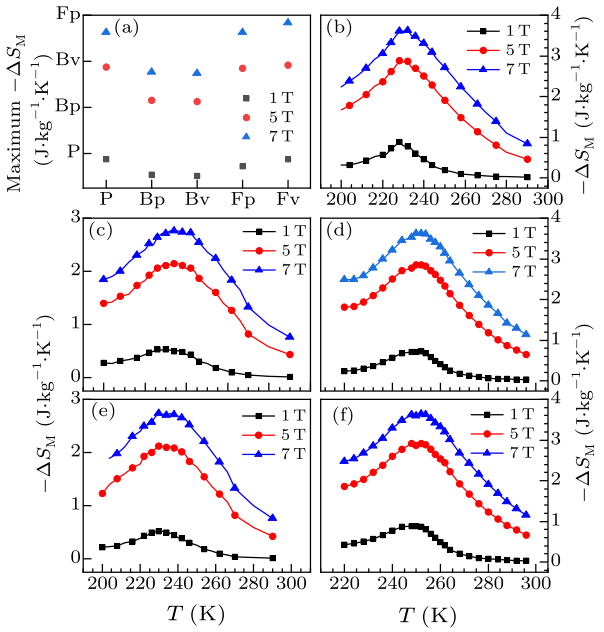

Fig. 4. (a) Maximum $-\Delta S_M$ for different samples with different applied magnetic fields. (b)–(f) Temperature dependence of magnetic entropy changes for different samples. Panels (b)–(f) correspond to samples P, Bp, Fp, Bv and Fv, respectively.

We measured the M–H curves of the samples at different temperatures and calculated $-\Delta S_M(T)$ using the Maxwell relations (see Fig. 4). The maximum $-\Delta S_M$ and the relative cooling power (RCP)[33,34] of different samples are listed in Table 2. RCP is calculated from the product of the maximum $|-\Delta S_M|$, and the full width at half maximum of the peak in entropy changes versus temperature. The maximum $-\Delta S_M$

and RCP for F are greater than those for B because of magnetocrystalline anisotropy. The sample Fv has the greatest maximum of $-\Delta S_{\rm M}$ and RCP, specifically, the greatest maximum of $-\Delta S_{\rm M}$ is 2.91 J·kg^{-1}K^{-1} (about one third of Gd) and 3.64 J·kg^{-1}K^{-1} at 5 and 7 T, and the corresponding RCPs are 212 and 302 J/kg, respectively. Accordingly, Fv has a considerable RCP and a wide working temperature (more than 80 K). However, the samples prepared by the same method show no significant difference in the maximum $-\Delta S_{\rm M}$ for a magnetic field applied in two mutually perpendicular directions, which indicates a small anisotropy. However, the RCP of sample Fv (212 J/kg at 5 T, and 302 J/kg at 7 T) exceeds that of sample Fp (174 J/kg at 5 T, and 286 J/kg at 7 T) because of the wider temperature span for sample Fv. In addition, the width of the peak in entropy change depends on the applied magnetic field, as the magnetic field ΔH increases, the width broadens. The properties make $Mn_{2-\delta}Sn$ a promising material for a large potential application in the magnetic refrigeration over a wide range of temperatures.

Table 2. Maximum $-\Delta S_{\rm M}$ and RCPs for different samples.

	Maximum $-\Delta S_{\rm M}$ (J·kg^{-1}·K^{-1})			RCP (J·kg^{-1})	
	$\Delta H = 1$ T	$\Delta H = 5$ T	$\Delta H = 7$ T	ΔH =5 T	$\Delta H = 7$ T
P	0.88	2.88	3.62	201	296
Bp	0.54	2.15	2.76	185	251
Bv	0.52	2.12	2.74	182	260
Fp	0.72	2.85	3.62	174	286
Fv	0.88	2.91	3.64	212	302

In summary, we have prepared single-phase polycrystalline and oriented samples of $Mn_{2-\delta}Sn$ alloys to study their magnetic properties. Almost all the samples undergo a re-entrant spin-glass-like transition and spin reorientation at low temperatures. The anisotropy of different oriented samples leads to different transition temperatures, saturation magnetizations, and maximum $-\Delta S_{\rm M}$. Sample Fv (applied magnetic field perpendicular to the [100] direction) is the easiest to magnetize and sample Bv (applied magnetic field perpendicular to the [101] direction) is the hardest to magnetize. The maximum magnetic entropy change also differs among different samples, and sample Fv has the largest value (maximum $-\Delta S_{\rm M}$ = 2.91 and 3.64 J·kg^{-1}K^{-1} with an applied magnetic field of 5 and 7 T, respectively). It also has the largest value of RCP (212 and 302 J/kg at 5 and 7 T, respectively). As the applied magnetic field ΔH increases, the maximum $-\Delta S_{\rm M}$ increases, which broadens the temperature range for refrigeration.

References

[1] Groot R A D, Mueller F M, Engen P G V and Buschow K H J 1983 *Phys. Rev. Lett.* **50** 2024
[2] Zutic I, Fabian J and Sarma S D 2004 *Rev. Mod. Phys.* **76** 323
[3] Felser C, Fecher G and Balke B 2007 *Angew. Chen. Int. Ed.* **46** 668
[4] Fujii S, Ishida S and Asano S 2010 *J. Phys. Soc. Jpn.* **79** 124702
[5] Yang C K, Zhao J J and Lu J P 2004 *Nano Lett.* **4** 561
[6] Osipov V V, Petukhov A G and Smelyanskiy V N 2005 *Appl. Phys. Lett.* **87** 202112
[7] Wang X T, Cheng Z X, Wang J L et al 2016 *J. Mater. Chem. C* **36** 8535
[8] Luo H Z, Liu G D, Meng F B et al 2011 *Physica B* **406** 4245
[9] Webster P J 1969 *Contemp. Phys.* **10** 559
[10] Kubler J, Williams A R and Sommers C B 1983 *Phys. Rev. B* **28** 1745
[11] Shaughnessy M, Fong C Y, Yang L H et al 2013 *J. Appl. Phys.* **113** 043709
[12] Alijani V, Meshcheriakova O, Winterlik J et al 2013 *J. Appl. Phys.* **113** 063904
[13] Kreiner G, Kalache A, Hausdorf S et al 2014 *Z. Anorg. Allg. Chem.* **640** 738
[14] Fuglsby R, Kharel P, Zhang W et al 2015 *J. Appl. Phys.* **117** 17D115
[15] Graf T, Felser C and Parkin S S P 2011 *Prog. Solid State Chem.* **39** 1
[16] Winterlik J, Chadov S, Gupta A et al 2012 *Adv. Mater.* **24** 6283
[17] Aprea C, Greco A, Maiorino A et al 2015 *J. Phys.: Conf. Ser.* **655** 01206
[18] Almanza M, Kedous-Lebouc A, Yonnet J P et al 2015 *Eur. Phys. J-Appl. Phys.* **71** 10903
[19] Silva D J, Bordalo B D, Puga J et al 2016 *Appl. Therm. Eng.* **99** 514
[20] Franco V, Blázquez J S, Ipus J J et al 2018 *Prog. Mater. Sci.* **93** 112
[21] Buschow K H J, van Engen P G and Jongebreur R 1983 *J. Magn. Magn. Mater.* **38** 1
[22] Vasilev E A and Gelyasin A E 1978 *Phys. Status Solidi* **47** K55
[23] Howotny H and Schubert K 1946 *Z. Metallkd.* **37** 17
[24] Kaplienko A I, Leonov B N and Chekin V V 1969 *Solid State Phys.* **11** 3030
[25] Satya M N S, Begum R J, Srinivasan B S et al 1965 *Phys. Lett.* **15** 223
[26] Shiraishi H, Hori T, Ohkubo N et al 2010 *Phys. Status Solidi* **1** 3660
[27] Yasukōchi K, Kanematsu K and Ohoyama T 1961 *J. Phys. Soc. Jpn.* **16** 1123
[28] Xu J H, Xia Y H, Yang W Y et al 2013 *J. Appl. Phys.* **113** 17E111
[29] Griffith G, Volkening F A and Claus H 1985 *J. Appl. Phys.* **57** 3392
[30] Dho J, Kim W S and Hur N H 2002 *Phys. Rev. Lett.* **89** 027202
[31] Hagiwara N, Matoba M, Fujii S et al 1993 *Phys. Status Solidi B* **176** K71
[32] Isogai Y, Kobayashi T, Yoshida T et al 1997 *Phys. Status Solidi* **203** 213
[33] Gschneidner K A and Jr. Pecharsky V K 2000 *Annu. Rev. Mater. Res.* **30** 387
[34] Xu J H, Yang W Y, Du Q H et al 2014 *J. Phys. D* **47** 065003